Interpreting the Coulomb-Field Approximation for Generalized-Born Electrostatics Using Boundary-Integral Equation Theory

Jaydeep P. Bardhan[1,2]

[1]*Mathematics and Computer Science Division*

Argonne National Laboratory, Argonne IL, USA

[2]*Department of Molecular Biophysics and Physiology*

Rush University, Chicago IL, USA

Abstract

The importance of molecular electrostatic interactions in aqueous solution has motivated extensive research into physical models and numerical methods for their estimation. In particular, the computational costs associated with simulations with explicit water have driven the development of implicit-solvent models, with generalized-Born (GB) models among the most popular of these. In this paper, we present a boundary-integral equation interpretation for the Coulomb-field approximation (CFA), which plays a central role in most GB models. This interpretation offers new insights into the nature of the CFA and its inaccuracies. In particular, it becomes clear that the CFA is most accurate when the molecular charge distribution generates a uniform normal displacement field at the solute–solvent boundary, and it is least accurate for distributions that give rise to rapidly varying or highly localized normal displacement fields. Supporting this analysis are comparisons of the reaction-potential matrices calculated using boundary-element-method (BEM) simulations and GB methods. We then introduce a similar approximation to the CFA that exhibits complementary behavior, with superior accuracy for charge distributions that generate rapidly varying normal fields and poorer accuracy for distributions that produce smooth fields. This approximation, which we call boundary-integral-based electrostatics estimation (BIBEE), is closely related to preconditioned Krylov-subspace iterative methods for BEM simulations. The presented CFA and BIBEE results suggest that improved electrostatics models may be obtained by exploiting the invariance of molecular charge distributions. The boundary-integral interpretation also leads naturally to methods to eliminate the interpolation inaccuracies associated with the Still equation, and may therefore have implications for electrostatic component analysis. Furthermore, iterative refinement of the BIBEE results recovers the BEM solution, and we show that excellent agreement can be obtained in only a few iterations. Finally, the boundary-integral-equation framework may provide a means to derive rigorous results explaining how the empirical correction terms in many modern GB models significantly improve accuracy in spite of their simple analytical form.

1. INTRODUCTION

The aqueous environment surrounding biological molecules significantly complicates theoretical and computational studies of inter- and intramolecular interactions [1–3]. Implicit-solvent models [3–8], which estimate a potential of mean force that the solvent exerts on a solute, are an attractive alternative to time-consuming simulations with explicit solvent [9–13]. Many implicit-solvent models treat electrostatic interactions using macroscopic continuum theory based on the Poisson–Boltzmann equation, which can be solved numerically [3, 4, 14–16]. However, because even these calculations generally demand a great deal of computational effort, still faster and more approximate models have been introduced for applications involving dynamics and rapid screening [17–21]. The generalized-Born (GB) model has become extremely popular for these purposes, in large part due to its agreement with more expensive PB calculations (see, for instance, [22]) and to the availability of high-quality implementations that can be employed in dynamics simulations [23–26]. Still *et al.* presented the original generalized-Born model [17], which approximates electrostatic interactions using effective Born radii that capture the degree to which the charges on solute atoms are screened by solvent. Pairwise energies are then evaluated according to an interpolation formula that recovers the correct self-energy for each atom (*i.e.*, at zero separation), and in the limit of infinite separation estimates the pairwise interaction as the interaction between isolated charges in solvent. The number of excellent reviews of generalized-Born models (see, *e.g.*, [27–29]) underscores the models' popularity, and no attempt will be made here to outline the field.

This paper analyzes one of the central assumptions employed in many GB models: the Coulomb-field approximation (CFA) introduced by Qiu *et al.* [23]. In the CFA, one assumes that when only a single nonzero charge resides in the actual solute cavity, the dominant contribution to the overall electrostatic free energy arises from the energy density integrated over the solute volume [30]. The CFA therefore usually leads to an expression for an atom's effective Born radius in terms of a volume integral over the solute volume. Ghosh *et al.* demonstrated that application of the divergence theorem allows the radius to be written instead in terms of a surface integral over the solute–solvent boundary [31], and noted that the CFA is exact for a spherical boundary with a single central charge. The inaccuracies associated with GB methods based on the CFA have led to several empirical

corrections [25, 30–34] that offer substantially improved agreement compared to more expensive simulations [35]. As Ghosh *et al.* noted, the surface-integration form of the CFA is closely related to a boundary-integral equation formulation for the electrostatic problem, which is known as the apparent-surface-charge (ASC) method or the polarizable-continuum model (PCM) [14, 15, 36].

The full extent of the relationship, and its attendant implications, do not appear to have been discussed previously, however. These details represent the main contribution of the present work. The shortcomings of the CFA are examined from the boundary-integral-equation perspective, which lends new insights into possibilities for improving approximate electrostatics models. We introduce an approximation that is entirely analogous to the CFA except that it is most accurate where the CFA is least accurate, and vice versa. This approximation, which is closely related to preconditioning methods for boundary-element method (BEM) simulations, forms the basis for an alternative approach to estimating free energies, the boundary-integral-based electrostatics estimation (BIBEE) method. The performance of the new approach is compared to GBMV [25] and the original Generalized-Born approach [23] using a surface formalism as in Ghosh *et al.* and Romanov *et al.* [30, 31]. High-resolution boundary-element-method (BEM) simulations of the continuum electrostatic model are used as reference calculations [37]. Modern GB methods like GBMV exhibit excellent agreement with Poisson–Boltzmann calculations that are hundreds or thousands of times more computationally expensive (for recent comparisons, see [25, 33, 35, 38–44]). To better highlight how current models may be improved further, we introduce a more discriminating comparison than is usually reported. Instead of comparing total electrostatic free energies calculated by different methods, we compare the reaction-potential matrices that they generate. The reaction-potential matrix offers a more detailed picture of the strengths and weaknesses of modeling assumptions and approximations.

The BIBEE technique exceeds the requirements of many modeling applications, and in its present form the model is unsuitable for dynamics, because it is not clear whether calculated forces are continuous functions of position. However, the method's theoretical foundations and accuracy suggest that further research in this direction is warranted. The primary goal of this research is to improve computationally efficient methods for reproducing more expensive simulations of the Poisson equation. Comparisons of GB calculations to explicit-solvent simulations are of interest as well [40, 45–48], but are beyond the scope of this

paper.

The following section presents the basic theoretical and numerical techniques used in this paper, including linear continuum-electrostatic theory for molecular solvation, boundary-integral formulations of the linear continuum problem, and the generalized-Born method for approximating electrostatic interactions. Section 3 describes the relation between the GB Coulomb-field approximation and integral equations, and illustrates the use of reaction-potential matrices as a more detailed means to compare methods for estimating electrostatic energies. Section 4 discusses the significance and implications of the present work. The final section summarizes the paper and suggests areas for future research.

2. THEORY

We consider the following linear-response continuum electrostatic model (extensive discussions of this model may be found in many reviews; see, *e.g.*, [3]). The solute and solvent regions are separated by a boundary Ω, which we take here to be the Richards and Connolly solvent-excluded (molecular) surface defined by rolling a probe sphere around the set of spheres that define the solute [49, 50]. The dielectric constant in the solute and solvent regions are denoted by ϵ_I and ϵ_{II}. The solute charge distribution $\rho(r)$ polarizes the solvent, which in turn creates a *reaction potential* in the solute. In this paper, $\rho(r)$ is assumed to be a set of m discrete point charges located at the sphere centers, and then the electrostatic free energy due to solvent polarization is $E = \frac{1}{2} q^T \varphi^{REAC}$, where q represents the m-length vector of point charge values and φ^{REAC} the vector of reaction potentials at the charge locations. Determining φ^{REAC} is the computational challenge in most calculations. We assume that the Poisson equation governs the potential in the solute, that the Laplace equation holds in the solvent, and that continuity and regularity conditions at Ω and infinity hold [51, 52]. Assuming linear response, the electrostatic response φ^{REAC} can be written as

$$\varphi^{REAC} = Mq, \tag{1}$$

where the symmetric and positive definite m-by-m matrix M is called the *reaction-potential matrix*. The following sections present boundary-element and generalized-Born methods for calculating M.

2.1. Boundary-Integral Formulations for Molecular Electrostatics

Boundary-element methods for solving this coupled PDE problem first convert it to boundary-integral-equation form, so that the unknowns are no longer the potential everywhere in space (as in finite-difference [4, 53, 54] or finite-element [55, 56] methods), but functions defined on the boundary Ω [8, 14–16, 52, 57–64]. In the popular apparent-surface-charge (ASC), or polarizable continuum model (PCM), formulation [14, 15, 36, 65], the unknown function is the polarization charge $\sigma_p(r)$ that develops at a dielectric interface in response to a field, and the integral equation can be written

$$\left(1 - \frac{\epsilon_I}{\epsilon_{II}}\right)\left(\frac{\partial}{\partial n(r)}\sum_{i=1}^{m}\frac{q_i}{4\pi||r-r_i||} + \frac{\partial}{\partial n(r)}\int_\Omega \frac{\sigma_p(r')}{4\pi||r-r'||}dA'\right) = \sigma_p(r), \tag{2}$$

Given the surface-charge distribution, the reaction potential φ^{REAC} at a charge location r_i is

$$\varphi^{REAC}(r_i) = \frac{1}{\epsilon_I}\int_\Omega \frac{\sigma_p(r')}{4\pi||r_i-r'||}dA'. \tag{3}$$

To solve (2) numerically, one may use the boundary-element method (BEM) [57]. For clarity, we present here only a simple BEM, approximating the boundary Ω with a set of n planar triangles, the unknown $\sigma_p(r)$ on Ω as a weighted combination of piecewise-constant basis functions defined on the boundary elements, and using accurate discretization techniques [65–67]. This process generates the finite-dimensional linear system

$$A_2 x = A_1 q, \tag{4}$$

in which the n-by-m matrix A_1 maps the vector of charge values, q, to the discretized form of the right-hand side of (2), A_2 is the n-by-n BEM matrix, and x is the vector of unknown basis-function weights. The diagonal entries of A_2 take the form

$$A_{2,ii} = \alpha_i\left(\frac{1}{2} - \left(1 - \frac{\epsilon_I}{\epsilon_{II}}\right)^{-1}\right), \tag{5}$$

where α_i is the area of boundary element i; more complete discussions of the discretization may be found in [65–67].

Using this discretization, the integral operator in (3), which maps the BEM approximation to $\sigma_p(r)$ to the reaction potentials at the charge locations, is transformed into an m-by-n matrix A_3, and thus the m-by-m reaction-potential matrix M can be expressed succinctly as

a product of three matrices: $M = A_3 A_2^{-1} A_1$. In typical electrostatic free energy calculations, one solves a single linear system by setting the elements of vector q to the desired values. The reaction-potential matrix M is usually calculated one column at a time (*e.g.*, for each atom i one sets $q_i = 1$ and the rest to zero) [68].

2.2. Generalized-Born Models

In the generalized-Born (GB) method [17, 23], M_{ij}, the pairwise energy between two unit charges i and j is defined by the Still equation

$$M_{ij} = \frac{1}{8\pi}\left(\frac{1}{\epsilon_{II}} - \frac{1}{\epsilon_I}\right)\frac{1}{\sqrt{r_{ij}^2 + R_i R_j \exp(-r_{ij}^2/4R_iR_j)}}, \tag{6}$$

where the parameters R_i and R_j, called *effective Born radii*, represent the degree of solvent screening seen by each charge. Each effective Born radius R_i is defined according to

$$R_i = \frac{1}{8\pi}\left(\frac{1}{\epsilon_{II}} - \frac{1}{\epsilon_I}\right)\frac{1}{E_i}, \tag{7}$$

where E_i, the *self-energy* of atom i, denotes the electrostatic free energy of the system when atom i has unit charge and the rest are neutral. Because the self-energies vary with the molecular geometry, dynamics or Monte Carlo methods based on GB electrostatics require very efficient methods for determining the E_i. Calculating effective radii using direct Poisson simulations produces energies that agree best with Poisson-calculated free energies [41]. However, such an approach clearly offers no reduction in computational cost, and therefore more inexpensive methods have been developed that calculate only approximate effective radii [23, 25, 26, 32, 33]. Other generalized-Born-like approaches, such as the pairwise descreening approximation (PDA) [69, 70], also exist.

A simplifying assumption that plays a central role in most GB methods is called the Coulomb-field approximation (CFA). In the CFA one assumes that R_i is a function of the volume integral of the energy density induced in a homogeneous dielectric, where the volume V is that of the solute volume enclosed by Ω:

$$R_i^{-1} = \frac{1}{(4\pi)^2}\int_V \frac{1}{||r_i - r'||^4} dV', \tag{8}$$

with related expressions typically used for convenient volume integration [71]. Ghosh *et al.* applied the divergence theorem to (8) to obtain a surface-integral expression for R_i [31]:

$$R_i^{-1} = \frac{1}{(4\pi)^2}\int_\Omega \frac{(r' - r_i)^T \hat{n}(r')}{||r' - r_i||^4} dA'. \tag{9}$$

Ghosh *et al.* noted that for a spherical solute with central charge at r_i, substituting (7) into (9) and solving for E_i produces an expression closely related to the ASC boundary-integral formulation (2). In particular, for this symmetric case, the total value of the boundary integral in (2) is zero and therefore the surface-charge density at any point r is exactly equal to the value of the charge-induced normal displacement field at r. The equivalence between the CFA volume and surface integrals then suggests that the CFA itself rests on the assumption that at every point on the boundary, the boundary integral evaluates to zero.

It is true that for a spherical boundary with one central charge, the total value of the surface integral in (2) equals zero, being equal to the jump in the normal displacement field (1/2) plus the principal value of the integral (−1/2) [51]. However, the crucial point that we wish to make in this paper is that the cancellation arises not from symmetry *per se* but from the fact that the actual distribution of induced charge is uniform everywhere, and will hold for any closed boundary. As Mongan *et al.* note, the CFA is exact for the sphere only if the charge is at the center, and the error between the CFA self-energy and the true self-energy approaches 100% as the charge approaches the surface [72]. It is the error in the CFA assumption of a uniform induced density that gives rise to this discrepancy. For highly non-spherical solutes like biomolecules, a single point charge almost never induces a uniform normal displacement field, and this fact motivates the examination of the reaction-potential matrix as a means to assess what determines the accuracy of the CFA.

The relationship between between the CFA surface integral (9) and the ASC integral equation holds even in the nonsymmetric case. As shown above, the CFA assumes that at any point r on Ω the local surface charge density $\sigma_p(r)$ is exactly equal to the normal displacement field induced by the solute charge distribution

$$\sigma_{p,CFA}(r) = \left(1 - \frac{\epsilon_I}{\epsilon_{II}}\right) \frac{\partial}{\partial n(r)} \sum_{i=1}^{m} \frac{q_i}{4\pi||r - r_i||}. \tag{10}$$

The resulting reaction potential at r_i in the solute is then

$$\varphi^{REAC}(r_i) = \left(\frac{1}{\epsilon_I} - \frac{1}{\epsilon_{II}}\right) \int_\Omega \left(\frac{1}{4\pi||r_i - r'||} \sum_{j=1}^{m} \frac{-(r' - r_j)^T \hat{n}(r')}{4\pi||r' - r_j||^3} \right) dA', \tag{11}$$

and the surface integral is equivalent to (9) if $m = 1$ and $q_1 = 1$. Note that (11) indicates that the same computational effort required for SGB methods [31] can give electrostatic energies directly, without use of the interpolative Still equation.

3. BOUNDARY-INTEGRAL-BASED ELECTROSTATICS ESTIMATION

We now detail how the uniform-normal-field assumption of the CFA affects the accuracy of GB/CFA methods, and how alternative approximations, with different regimes of accuracy, suggest that future electrostatic models may be improved on a physically rigorous basis.

We use as a model problem the neutral tripeptide Ala-Tyr-Phe with acetylated N-terminal and N-methylamide C-terminal blocking groups. The molecular-mechanics program CHARMM [73] (version 34a1) was used to generate the tripeptide, with the geometry used as built. This 56-atom molecule has sufficient complexity to demonstrate that the analysis applies to nontrivial surfaces, yet has a small enough reaction-potential matrix M to allow methods to be compared by visual inspection. All calculations employed CHARMM22 [74] radii and charges, a probe radius of 1.4 Å, $\epsilon_I = 1$, and $\epsilon_{II} = 80$. The program MSMS [75] was used to generate planar boundary-element representations of the Connolly molecular surface, at a vertex density of $20/\text{Å}^2$; the resulting discretization consisted of 15212 triangular boundary elements. The FFTSVD fast solver was used to solve the BEM problems and determine the radii used for SGB-based calculations [37, 76]. The BEM-based reaction-potential matrices were calculated using preconditioned GMRES [77] with a tolerance of 10^{-4}. Calculations using the GBMV module [25, 34, 35] used grid-based integration to determine radii and energies. All eigenvalue decompositions

$$M = V \Lambda V^T, \tag{12}$$

where V is the matrix whose columns are the eigenvectors of M and Λ is the diagonal matrix with diagonal entries equal to the corresponding eigenvalues of M, were computed with MATLAB [78]. Because the eigendecomposition explicitly details the shape and curvature of the electrostatic free energy, which is a quadratic function of the m charges, it enables more fine-grained assessments of the strengths and weaknesses of different electrostatic models.

Figure 1(a) is a plot of the magnitudes of the eigenvalues of the BEM-calculated reaction-potential matrix M_{BEM}; throughout the text, the subscript on a reaction-potential matrix denotes the method by which it was calculated. Figure 1(b) contains plots of the eigenvectors associated with λ_1, λ_2, λ_{20}, and λ_{40}; as can be seen in the Figure, the eigenvector V_1 represents a relatively homogeneous charge distribution. This distribution generates an approximately uniform normal displacement field at the boundary, as can be seen in Figure 2(a).

Eigenvectors associated with smaller-magnitude eigenvalues represent charge distributions that generate progressively less smooth and more rapidly varying normal displacement fields. Figure 2(b) is a plot of the normal displacement field if the charge distribution $q = V_2$, illustrating that the eigenvector generates a normal field resembling that of a dipole. In contrast, the normal displacement fields generated by the eigenvectors that correspond to much smaller eigenvalues are highly localized, with the normal displacement very near zero over most of the surface. This can be seen in Figure 2(c) and (d), which are plots of the induced normal displacement field when $q = V_{20}$ and $q = V_{40}$.

The dependence of the CFA on the assumption of a uniform distribution of induced charge can be assessed by comparing the eigendecomposition of the SGB/CFA reaction-potential matrix M_{CFA} to that of the boundary-element reaction-potential matrix M_{BEM}. As shown in Figure 3(a), the largest-magnitude approximate eigenvalues match very closely those of the more accurate simulations. Also, from Figure 3(b), which is a plot of the magnitudes of the entries of

$$S = V_{BEM}^T V_{CFA}, \tag{13}$$

which is the projection of V_{CFA} onto V_{BEM}. The magnitude of the matrix entry S_{ij} therefore represents the degree to which eigenvector j of the approximate reaction-potential matrix is aligned with that of eigenvector i of M_{BEM}. Perfect alignment between the eigenvectors of V_{CFA} and V_{BEM} would produce a matrix with zeros on the off-diagonal entries; conversely, nonzero values off the diagonal indicate imperfect alignment. It can be seen that just as with the largest-magnitude eigenvalues, the dominant eigenvectors of M_{CFA} and M_{BEM} agree well, with the quality of approximation deteriorating for smaller eigenvalues.

A different diagonal approximation, which we now detail, produces complementary behavior, with excellent agreement for the eigenvalues of smallest magnitude. This alternative approach is based on diagonal preconditioning of the BEM linear systems. Because BEM matrices are dense—*i.e.*, they generally have no non-zero entries—explicitly forming a BEM matrix and factorizing it with Gaussian elimination is impractical for a problem with more than several thousand unknowns. Alternative techniques, known as Krylov-subspace iterative methods, are therefore typically employed to solve the linear systems approximately. Methods such as the conjugate gradient method (CG) and GMRES [77] solve, at iteration j, the BEM matrix equation $A_2 x = A_1 q$ approximately, choosing an approximate solution

$\hat{x}^j$ that lies in the subspace

$$A_1 q, A_2 A_1 q, \ldots, A_2^{j-1} A_1 q. \tag{14}$$

The iteration is terminated when the residual $||A_1 q - A_2 \hat{x}^j||$ is less than a specified tolerance ϵ_{TOL}.

Noting that the application of the integral operator A_2 entails the calculation of the potential (more precisely, its gradient) due to a set of n sources, it is clear that algorithms like the fast-multipole method [59, 64, 79, 80] can be used to calculate the needed matrix–vector products in $O(n)$ time rather than the $O(n^2)$ time normally required for dense matrix–vector multiplication. To further reduce computational effort, *preconditioning* is often employed to reduce the total number of matrix–vector products required to reach the specified tolerance. Preconditioned Krylov iterative methods solve the linear system $PA_2 x = Pb$, where the preconditioner matrix P is designed so that it may be applied rapidly and so that the eigenvalues of PA_2 are more tightly clustered than those of A_2 [81]. The diagonal matrix entries of discretized electrostatic integral operators are typically significantly larger in magnitude than the off-diagonal entries, and therefore diagonal preconditioners with $P_{ii} = A_{2,ii}^{-1}$ are often very effective [61, 65, 82, 83].

Because P is a reasonable approximation to A_2^{-1}, we define the approximate reaction-potential matrix

$$M_{B-0} = A_3 P A_1, \tag{15}$$

to be the 0-step BIBEE method, because zero applications of the operator A_2 are required. Figure 4(a) and 4(b) allow a comparison between M_{BEM} and M_{B-0}.

The 0-step BIBEE reaction-potential matrix has eigenvalues that closely match those of M_{BEM} for the smallest-magnitude eigenvalues, and are increasingly inaccurate for larger eigenvalues. This phenomenon arises because the diagonal entries of the BEM matrix include the discontinuity of $\frac{1}{2}$ in the normal displacement field but neglect the field due to the surface charge density elsewhere on the surface. Thus, both the CFA and 0-step BIBEE methods include first-order corrections to the effects of the charge distribution on the rest of the boundary. Whereas the CFA assumes a uniform distribution and thus a contribution of $-\frac{1}{2}$ from the remainder of the boundary, the 0-step BIBEE method assumes zero contribution. The methods' complementary performance in different regions of the spectrum illustrates that the quality of these corrections depends on the details of the charge distribu-

tion. One may also design a preconditioner that uses the CFA normalization instead of the BEM normalization. The resulting reaction-potential matrix $\hat{M}_{B-0/CFA}$ compares similarly to M_{BEM} as does M_{CFA}, as can be seen by comparing Figure 3(a) and Figure 4(a); the eigenvalues of largest magnitude are matched well, with the approximation decreasing in quality for smaller eigenvalues. The eigenvectors of M_{B-0} and $M_{B-0/CFA}$ are almost identical (data not shown), which suggests that the misalignment of the eigenvectors of M_{CFA} relative to those of M_{BEM} may arise due to the GB interpolation.

The 0-step calculations may be refined iteratively, and will eventually converge to the full BEM solution. Writing

$$A_2 = D - E, \tag{16}$$

where $D = P^{-1}$ and E has zeros on the diagonal and $E_{ij} = -A_{2,ij}$ otherwise. The preconditioned linear system is then

$$(I - PE)x = PA_1q, \tag{17}$$

and refined approximations may be found using the k-term truncated Neumann series approximations to $(I - PE)^{-1}$:

$$x \approx (I + PE + (PE)^2 + \ldots + (PE)^k)PA_1q. \tag{18}$$

The k^{th} iterate of the Krylov-subspace iterative method GMRES [77] uses the same basis vectors as the $k-1$-term truncated Neumann-series expansion, as can be seen by comparing (14) and (18), but weights the basis vectors differently [57].

We now describe a physical interpretation for the refinement process, neglecting preconditioning for clarity. At any point r on the surface, the dominant contribution to the normal electric-displacement field arises from the surface-charge density σ_p at r. Thus, in the first-order approximation one neglects completely the field induced by σ_p elsewhere on the boundary. The second- and higher-order terms may be accounted for, approximately, by successively calculating the normal displacement field induced at r by the off-diagonal entries given the approximate σ_p already obtained. The extra surface charge induced at r is then determined by applying the inverse of the diagonal component of the total integral operator. This type of refinement is therefore related to what is known the integral equation literature as the method of iteration [57].

The 1- and 2-step BIBEE methods are obtained by using one and two GMRES iterations to obtain refined estimates of the surface charge distribution, and the corresponding reaction-

potential matrices M_{B-1} and M_{B-2}. Their eigenvalues and eigenvectors are compared to those of M_{BEM} in Figures 5 and 6. The failure of the 1-step method to achieve even comparable results to the 0-step method may be due to the means by which Krylov-subspace iterative methods find approximate solutions. Neglecting preconditioning, the i^{th} iteration of GMRES chooses a polynomial of degree $i-1$ in A_2, $p(A_2)$, that minimizes the norm of the residual $||p(A_2)A_1q||$ [81]. Whereas 0-step BIBEE does not involve a polynomial at all, and the 2-step method can use complex conjugate roots, the 1-step method must choose a single real root. Although the residual must decrease as basis vectors are added to the subspace from which the approximate solution is found, the actual energetics associated with the approximate surface-charge distribution may not improve if the actual characteristic polynomial of A_2 is poorly approximated. This seems plausible because the electric-field kernel is antisymmetric and therefore has complex eigenvalues, but further research is needed to establish this connection more definitively.

The GBMV module of CHARMM was employed to compare the BIBEE methods to modern GB methods, which employ empirical correction terms beyond the CFA. Figure 7(a) and (b) are plots of the M_{GBMV} eigenvalues and the projections of its eigenvectors onto those of M_{BEM}. It is clear that the empirical correction terms in GBMV improve the eigenvalue estimates relative to those of the purely CFA-based M_{CFA}.

4. DISCUSSION

The alignment of the eigenvectors between approximate methods and the more expensive reference calculation has physical meaning. Assuming that the approximate eigenvalues exactly equal those of the reference calculation, misalignment of the eigenvectors corresponds to a rotation of the energy landscape in charge space, relative to the reference landscape. Consequently, component analysis based on an electrostatics method known to produce inaccurate eigenvectors may generate misleading or incorrect results. Second, although GBMV produces clearly superior eigenvalue approximations compared to SGB/CFA, the similarity of the projections of V_{GBMV} and V_{CFA} onto V_{BEM} suggests that the SGB/CFA and GBMV models have at least one weakness in common. It is possible that these weaknesses result from the interpolation associated with the Still equation. It may be that the misalignment of eigenvectors despite the presence of good eigenvalue estimates is responsible for the seem-

ingly conflicting results found in the literature; some authors note that GB and PB methods calculate very similar energies ([22, 39, 40]) and others report that GB methods fail to accurately reproduce certain energy landscapes [42, 84–86]. Because the simple 0-step BIBEE calculation gives rise to a reaction-potential matrix with eigenvectors that are much better aligned with the reference calculation, and are, surprisingly, better aligned than those from GBMV, investigations that employ component analysis may benefit from BIBEE.

Section 3 demonstrated that the 0-step method and the SGB/CFA method both calculate m surface integrals, with the methods employing only slightly different integrands. First, as discussed, the methods scale the induced normal displacement field by different constants. Second, the SGB/CFA method places a unit charge on each atom in succession, using the resulting surface integral to determine the corresponding effective Born radius, and then these radii are used in the Still equation. In contrast, the 0-step BIBEE method sets all charges to the appropriate values, with the resulting approximation to the surface charge density used to calculate the reaction potentials at the m charge locations. Although m surface integrations are required for a naive implementation, fast-multipole methods can accelerate the calculation so that these integrations are performed simultaneously. Thus, as mentioned in Section 2, surface-integration GB methods already implemented can be modified to eliminate the need for the Still equation, if energies rather than forces are to be calculated; the treatment of dynamics is more complex and not yet resolved.

The higher-order terms associated with the series expansion for the iterative refinements may be related to the empirical corrections used in modern generalized-Born methods [25, 26, 30, 32, 33]. It is intriguing that GBMV, which is one of the most recently developed GB methods, exhibits improved correspondence to the BEM calculations near the middle of the spectrum. It is possible that the GBMV corrections are especially well-suited for correcting the errors in the CFA given charge distributions such as those found in the corresponding eigenvectors. Finally, in most calculations with nonpolarizable force fields, the atomic charges remain constant, and this invariance has not yet to be exploited computationally. A simple method might be to use multi-step BIBEE infrequently to accurately estimate the influence of the remainder of the surface charge, with updates based on 0-step BIBEE applied in between more accurate BIBEE calculations. This type of approach would enable accurate inclusion of nonlocal solvent-polarization forces without sacrificing computational efficiency. Not only dynamics, but also Monte Carlo methods [18, 87, 88]

and protein engineering calculations [89, 90] could benefit from such a strategy.

5. SUMMARY

This paper has used a boundary-integral-equation framework to analyze the Coulomb-field approximation (CFA) that plays a major role in most generalized-Born (GB) models for molecular electrostatics in aqueous environments. It has been shown that the CFA implicitly assumes that the solute charge distribution generates a uniform normal displacement field on the boundary. A simple model problem illustrates that this assumption holds for some types of charge distributions but not all, and that some charge distributions are poorly treated with the CFA. A slightly different technique, BIBEE, has also been presented in the boundary-integral framework, and shown to exhibit a complementary relationship between the charge distribution and resulting accuracy. The BIBEE method also allows straightforward refinement towards a rigorous solution to the electrostatic problem, without recourse to empirical corrections. The reaction-potential matrix has been used as a means to compare electrostatics simulation methods such as GB and BIBEE. In this paper the eigendecomposition has been used exclusively, but alternative projection schemes may be useful for component analysis and for investigating the relationships between problem geometry, electrostatic model, and simulation accuracy. To study these relationships and the previously reported shortcomings of the GB approach[13, 38, 42, 84–86, 91, 92], future studies will compare the reaction-potential matrices generated by modern GB techniques and standard approaches to simulating electrostatics.

Clearly, many issues remain to be addressed before BIBEE can be a viable approach for general use. One obvious advantage of existing GB and GB-like methods is that they may be used for dynamics. Refining BIBEE to enable its use in dynamics is therefore a primary goal of current research. Fast-multipole methods [59, 79], which have a long history in biophysical simulations [93–96] offer an attractive route, although significant complications may arise if current approximations to the solute–solvent interface (see, for instance, [34]) are not amenable to rapid, and easily updated, surface discretization. However, Totrov and Abagyan have already demonstrated a simplified boundary-element method used in Monte Carlo simulations of peptide folding, using their fast contour-buildup algorithm to discretize the surface [21, 97]. The BIBEE method follows their approach in retaining a

high-resolution discretization of the solute–solvent interface and only later approximating solution of the BEM problem itself; it has been noted that accurate representation of the dielectric boundary is important for obtaining high-quality electrostatic energies [98].

In this paper, a diagonal preconditioner has been used to elucidate the connection between boundary-integral equation methods for electrostatics and the generalized-Born method. Such a preconditioner allows the development of a simple BIBEE method that requires a small number of matrix–vector products. Many other preconditioners have been described in the boundary-element method literature [83], including the $\mathcal{H}$-matrices introduced by Hackbusch *et al.* [99–101] and overlap preconditioners [102]. Their use may permit superior approximations to the calculations presented here. Furthermore, alternative second-kind integral-equation formulations of the electrostatic problem, like that of Juffer *et al.* [52], allow treatment of problems in which the linearized Poisson–Boltzmann equation is used to model the potential in the solvent region. An analogous approach to BIBEE can be employed for that formulation as well, which would give rise a rigorous approach to GB-like electrostatics in ionic solutions [103, 104].

It is also of interest to investigate whether the boundary-integral interpretation may be used to analyze membrane GB models [29, 105, 106], and whether it is related to recent work by Egwolf and Tavan [107, 108]. It has been noted that some of the deficiencies of purely implicit-solvent models are endemic and that improved methods are warranted [109]. We hope that the present analysis may eventually be useful for the refinement of hybrid models that use explicit solvation-shell waters and implicit water elsewhere [88, 110–114].

ACKNOWLEDGMENTS

The author thanks B. Roux for the use of CHARMM and for encouragement, M. Anitescu, M. K. Gilson, and D. F. Green for valuable discussions, and gratefully acknowledges funding from a Wilkinson Fellowship in Scientific Computing funded by the Mathematical, Information, and Computational Sciences Division Subprogram of the Office of Advanced Scientific Computing Research, Office of Science, U. S. Dept. of Energy, under Contract DE-AC02-06CH11357. The author would also like to acknowledge the support and hospitality of the Radon Institute for Computational and Applied Mathematics (RICAM) at the

Johannes Kepler Universität in Linz, Austria, where a portion of this work was conducted.

---

[1] J. G. Kirkwood. Theory of solutions of molecules containing widely separated charges with special application to zwitterions. *Journal of Chemical Physics*, 2:351, 1934.

[2] C. Tanford and J. G. Kirkwood. Theory of protein titration curves I. General equations for impenetrable spheres. *Journal of the American Chemical Society*, 59:5333–5339, 1957.

[3] K. A. Sharp and B. Honig. Electrostatic interactions in macromolecules: Theory and applications. *Annual Review of Biophysics and Biophysical Chemistry*, 19:301–332, 1990.

[4] J. Warwicker and H. C. Watson. Calculation of the electric potential in the active site cleft due to alpha-helix dipoles. *Journal of Molecular Biology*, 157:671–679, 1982.

[5] B. Roux and T. Simonson. Implicit solvent models. *Biophysical Chemistry*, 78:1–20, 1999.

[6] C. J. Cramer and D. G. Truhlar. Implicit solvation models: Equilibria, structure, spectra, and dynamics. *Chemical Reviews*, 99:2161–2200, 1999.

[7] M. Orozco and F. J. Luque. Theoretical methods for the description of the solvent effect in biomolecular systems. *Chemical Reviews*, 100:4187–4225, 2000.

[8] T. Simonson. Macromolecular electrostatics: Continuum models and their growing pains. *Current Opinions in Structural Biology*, 11:243–252, 2001.

[9] V. Lounnas, B. M. Pettitt, L. Findsen, and S. Subramaniam. A microscopic view of protein solvation. *Journal of Physical Chemistry*, 18:7157–7159, 1992.

[10] J. A. McCammon and S. C. Harvey. *Dynamics of Proteins and Nucleic Acids*. Cambridge University Press, Cambridge, 1987.

[11] C. L. Brooks, III, M. Karplus, and B. M Pettitt. Proteins: A theoretical perspective of dynamics, structure and thermodynamics. *Advances in Chemical Physics*, 71:1–249, 1988.

[12] S. W. Rick and B. J. Berne. The aqueous solvation of water: A comparison of continuum methods with molecular dynamics. *Journal of the American Chemical Society*, 116:3949–3954, 1994.

[13] M. Shen and K. F. Freed. Long time dynamics of Met-Enkephalin: Comparison of explicit and implicit solvent models. *Biophysical Journal*, 82:1791–1808, 2002.

[14] P. B. Shaw. Theory of the Poisson Green's-function for discontinuous dielectric media with an application to protein biophysics. *Physical Review A*, 32:2476–2487, 1985.

[15] R. J. Zauhar and R. S. Morgan. The rigorous computation of the molecular electric potential. *Journal of Computational Chemistry*, 9:171–187, 1988.

[16] E. O. Purisima and S. H. Nilar. A simple yet accurate boundary-element method for continuum dielectric calculations. *Journal of Computational Chemistry*, 16:681–689, 1995.

[17] W.C. Still, A. Tempczyk, R. C. Hawley, and T. F. Hendrickson. Semianalytical treatment of solvation for molecular mechanics and dynamics. *Journal of the American Chemical Society*, 112:6127–6129, 1990.

[18] D. Horvath, D. vanBelle, G. Lippens, and S. J. Wodak. Development and parametrization of continuum solvent models .1. Models based on the boundary element method. *Journal of Chemical Physics*, 104:6679–6695, 1996.

[19] P. F. B. Gonçalves and H. Stassen. New approach to free energy of solvation applying continuum models to molecular dynamics simulation. *Journal of Computational Chemistry*, 23:706–714, 2002.

[20] R. Luo, L. David, and M. K. Gilson. Accelerated Poisson–Boltzmann calculations for static and dynamic systems. *Journal of Computational Chemistry*, 23:1244–1253, 2002.

[21] M. Totrov and R. Abagyan. Rapid boundary element solvation electrostatics calculations in folding simulations: Successful folding of a 23-residue peptide. *Biopolymers*, 60:124–133, 2001.

[22] M. Feig, A. Onufriev, M. S. Lee, W. Im, D. A. Case, and C. L. Brooks III. Performance comparison of generalized Born and Poisson methods in the calculation of electrostatic solvation energies for protein structures. *Journal of Computational Chemistry*, 25:265–284, 2004.

[23] D. Qiu, P. S. Shenkin, F. P. Hollinger, and W. C. Still. The GB/SA continuum model for solvation. A fast analytical method for the calculation of approximate Born radii. *Journal of Physical Chemistry A*, 101:3005–3014, 1997.

[24] B. N. Dominy and C. L. Brooks III. Development of a generalized Born model parametrization for proteins and nucleic acids. *Journal of Physical Chemistry B*, 103:3765–3773, 1999.

[25] M. S. Lee, F. R. Salsbury, and C. L. Brooks III. Novel generalized Born methods. *Journal of Chemical Physics*, 116:10606–10604, 2002.

[26] W. Im, M. S. Lee, and C. L. Brooks III. Generalized Born method with a simple smoothing function. *Journal of Computational Chemistry*, 24:1691–1702, 2003.

[27] D. Bashford and D. A. Case. Generalized Born models of macromolecular solvation effects.

Annual Review of Physical Chemistry, 51:129–152, 2000.

[28] N. A. Baker. Improving implicit solvent simulations: A Poisson-centric view. *Current Opinions in Structural Biology*, 15:137–143, 2005.

[29] M. Feig, J. Chocholoušová, and S. Tanizaki. Extending the horizon: Towards the efficient modeling of large biomolecular complexes in atomic detail. *Theoretical Chemistry Accounts*, 116:194–205, 2006.

[30] A. N. Romanov, S. N. Jabin, Y. B. Martynov, A. V. Sulimov, F. V. Grigoriev, and V. B. Sulimov. Surface generalized Born method: A simple, fast, and precise implicit solvent model beyond the Coulomb approximation. *Journal of Physical Chemistry A*, 108:9323–9327, 2004.

[31] A. Ghosh, C. S. Rapp, and R. A. Friesner. Generalized Born model based on a surface integral formulation. *Journal of Physical Chemistry B*, 102:10983–10990, 1998.

[32] T. Grycuk. Deficiency of the Coulomb-field approximation in the generalized Born model: An improved formula for Born radii evaluation. *Journal of Chemical Physics*, 119:4817–4826, 2003.

[33] M. Wojciechowski and B. Lesyng. Generalized Born model: Analysis, refinement, and applications to proteins. *Journal of Physical Chemistry B*, 108:18368–18376, 2004.

[34] M. S. Lee, M. Feig, F. R. Salsbury, and C. L. Brooks III. New analytic approximation to the standard molecular volume definition and its application to generalized Born calculations. *Journal of Computational Chemistry*, 24:1348–1356, 2003.

[35] M. Feig and C. L. Brooks III. Recent advances in the development and application of implicit solvent models in biomolecule simulations. *Current Opinions in Structural Biology*, 14:217–224, 2004.

[36] S. Miertus, E. Scrocco, and J. Tomasi. Electrostatic interactions of a solute with a continuum – a direct utilization of *ab initio* molecular potentials for the prevision of solvent effects. *Chemical Physics*, 55:117–129, 1981.

[37] M. D. Altman, J. P. Bardhan, J. K. White, and B. Tidor. Accurate solution of multi-region continuum electrostatic problems using the linearized Poisson–Boltzmann equation and curved boundary elements. *(in press, Journal of Computational Chemistry).*

[38] S. R. Edinger, C. Cortis, P. S. Shenkin, and R. A. Friesner. Solvation free energies of peptides: Comparison of approximate continuum solvation models with accurate solution of the Poisson–Boltzmann equation. *Journal of Physical Chemistry B*, 101:1190–1197, 1997.

[39] L. David, R. Luo, and M. K. Gilson. Comparison of Generalized Born and Poisson models: Energetics and dynamics of HIV protease. *Journal of Computational Chemistry*, 21:295–309, 2000.

[40] L. Y. Zhang, E. Gallicchio, R. A. Friesner, and R. M. Levy. Solvent models for protein-ligand binding: Comparison of implicit solvent Poisson and surface generalized Born models with explicit solvent simulations. *Journal of Computational Chemistry*, 22:591–607, 2001.

[41] A. Onufriev, D. A. Case, and D. Bashford. Effective Born radii in the generalized Born approximation: The importance of being perfect. *Journal of Computational Chemistry*, 23:1297–1304, 2002.

[42] J. Zhu, E. Alexov, and B. Honig. Comparative study of generalized Born models: Born radii and peptide folding. *Journal of Physical Chemistry B*, 109:3008–3022, 2005.

[43] G. Sigalov, A. Fenley, and A. Onufriev. Analytical electrostatics for biomolecules: Beyond the generalized Born approximation. *Journal of Chemical Physics*, 124(124902), 2006.

[44] J. Mongan, C. Simmerling, J. A. McCammon, D. A. Case, and A. Onufriev. Generalized Born model with a simple, robust molecular volume correction. *Journal of Chemical Theory and Computation*, 3:156–169, 2007.

[45] B. Xia, V. Tsui, D. A. Case, H. Jane Dyson, and P. E. Wright. Comparison of protein solution structures refined by molecular dynamics simulation in vacuum, with a generalized Born model, and with explicit water. *Journal of Biomolecular NMR*, 22:317–331, 2002.

[46] H. Nymeyer and A. E.García. Simulation of the folding equilibrium of α-helical peptides: A comparison of the generalized Born approximation with explicit solvent. *Proceedings of the National Academy of Sciences of the USA*, 100:13934–13939, 2003.

[47] Z. A. Sands and C. A. Laughton. Molecular dynamics simulations of DNA using the generalized Born solvation model: Quantitative comparisons with explicit solvation results. *Journal of Physical Chemistry B*, 108:10113–10119, 2004.

[48] M. S. Formaneck and Q. Cui. The use of a generalized Born model for the analysis of protein conformational transitions: A comparative study with explicit solvent simulations for Chemotaxis Y protein (CheY). *Journal of Computational Chemistry*, 27:1923–1943, 2006.

[49] F. M. Richards. Areas, volumes, packing, and protein structure. *Annual Review of Biophysics and Bioengineering*, 6:151–176, 1977.

[50] M. L. Connolly. Analytical molecular surface calculation. *Journal of Applied Crystallography*,

16:548–558, 1983.

[51] J. D. Jackson. *Classical Electrodynamics*. Wiley, 3^{rd} edition, 1998.

[52] A. H. Juffer, E. F. F. Botta, B. A. M. van Keulen, A. van der Ploeg, and H. J. C. Berendsen. The electric potential of a macromolecule in a solvent: A fundamental approach. *Journal of Computational Physics*, 97:144–171, 1991.

[53] M. K. Gilson, A. Rashin, R. Fine, and B. Honig. On the calculation of electrostatic interactions in proteins. *Journal of Molecular Biology*, 183:503–516, 1985.

[54] J. D. Madura, J. M. Briggs, R. C. Wade, M. E. Davis, B. A. Luty, A. Ilin, J. Antosiewicz, M. K. Gilson, B. Bagheri, L. Ridgway-Scott, and J. A. McCammon. Electrostatics and diffusion of molecules in solution: Simulations with the University of Houston Brownian Dynamics program. *Computer Physics Communications*, 91:57–95, 1995.

[55] C. M. Cortis and R. A. Friesner. Numerical solution of the Poisson–Boltzmann equation using tetrahedral finite-element meshes. *Journal of Computational Chemistry*, 18:1591–1608, 1997.

[56] N. A. Baker, D. Sept, M. J. Holst, and J. A. McCammon. Electrostatics of nanoysystems: Application to microtubules and the ribosome. *Proceedings of the National Academy of Sciences of the USA*, 98:10037–10041, 2001.

[57] K. E. Atkinson. *The Numerical Solution of Integral Equations of the Second Kind*. Cambridge University Press, 1997.

[58] B. J. Yoon and A. M. Lenhoff. A boundary element method for molecular electrostatics with electrolyte effects. *Journal of Computational Chemistry*, 11:1080–1086, 1990.

[59] R. Bharadwaj, A. Windemuth, S. Sridharan, B. Honig, and A. Nicholls. The fast multipole boundary-element method for molecular electrostatics: An optimal approach for large systems. *Journal of Computational Chemistry*, 16:898–913, 1995.

[60] J. Liang and S. Subramaniam. Computation of molecular electrostatics with boundary element methods. *Biophysical Journal*, 73:1830–1841, 1997.

[61] S. S. Kuo, M. D. Altman, J. P. Bardhan, B. Tidor, and J. K. White. Fast methods for simulation of biomolecule electrostatics. In *International Conference on Computer Aided Design (ICCAD)*, 2002.

[62] A. H. Boschitsch, M. O. Fenley, and H.-X. Zhou. Fast boundary element method for the linear Poisson–Boltzmann equation. *Journal of Physical Chemistry B*, 106:2741–54, 2002.

[63] A. J. Bordner and G. A. Huber. Boundary element solution of the linear Poisson–Boltzmann equation and a multipole method for the rapid calculation of forces on macromolecules in solution. *Journal of Computational Chemistry*, 24:353–367, 2003.

[64] B. Z. Lu, X. L. Cheng, J. Huang, and J. A. McCammon. Order N algorithm for computation of electrostatic interactions in biomolecular systems. *Proceedings of the National Academy of Sciences of the USA*, 103:19314–19319, 2006.

[65] M. D. Altman, J. P. Bardhan, J. K. White, and B. Tidor. An efficient and accurate surface formulation for biomolecule electrostatics in non-ionic solution. In *Engineering in Medicine and Biology Conference (EMBC)*, 2005.

[66] J. Tausch, J. Wang, and J. White. Improved integral formulations for fast 3-D method-of-moment solvers. *IEEE Transactions on Computer-Aided Design of Integrated Circuits and Systems*, 20:1398–1405, 2001.

[67] J. P. Bardhan. Numerical solution of boundary integral equations for molecular electrostatics. *Submitted to the Journal of Chemical Physics*.

[68] L.-P. Lee and B. Tidor. Barstar is electrostatically optimized for tight-binding to barnase. *Nature Structural Biology*, 8:73–76, 2001.

[69] G. D. Hawkins, C. J. Cramer, and D. G. Truhlar. Pairwise solute descreening of solute charges from a dielectric medium. *Chemical Physics Letters*, 246:122–129, 1995.

[70] G. D. Hawkins, C. J. Cramer, and D. G. Truhlar. Parametrized models of aqueous free energies of solvation based on pairwise descreening of solute atomic charges from a dielectric medium. *Journal of Physical Chemistry A*, 100:19824–19839, 1996.

[71] A. Onufriev, D. Bashford, and D. A. Case. Modification of the generalized Born model suitable for macromolecules. *Journal of Physical Chemistry B*, 104:3712–3720, 2000.

[72] J. Mongan, W. A. Svrcek-Seiler, and A. Onufriev. Analysis of integral expressions for effective Born radii. *Journal of Chemical Physics*, 127(185101), 2007.

[73] B. R. Brooks, R. E. Bruccoleri, B. D. Olafson, D. J. States, S. Swaminathan, and M. Karplus. CHARMM: A program for macromolecular energy, minimization, and dynamics calculations. *Journal of Computational Chemistry*, 4:187–217, 1983.

[74] A. D. MacKerell Jr., D. Bashford, M. Bellott, R. L. Dunbrack Jr., J. D. Evanseck, M. J. Field, S. Fischer, J. Gao, H. Guo, S. Ha, D. Joseph–McCarthy, L. Kuchnir, K. Kuczera, F. T. K. Lau, C. Mattos, S. Michnick, T. Ngo, D. T. Nguyen, B. Prodhom, W. E. Reiher III,

B. Roux, M. Schlenkrich, J. C. Smith, R. Stote, J. Straub, M. Watanabe, J. Wiorkiewicz–Kuczera, D. Yin, and M. Karplus. All-atom empirical potential for molecular modeling and dynamics studies of proteins. *Journal of Physical Chemistry B*, 102:3586–3616, 1998.

[75] M. Sanner, A. J. Olson, and J. C. Spehner. Reduced surface: An efficient way to compute molecular surfaces. *Biopolymers*, 38:305–320, 1996.

[76] M. D. Altman, J. P. Bardhan, B. Tidor, and J. K. White. FFTSVD: A fast multiscale boundary-element method solver suitable for BioMEMS and biomolecule simulation. *IEEE Transactions on Computer-Aided Design of Integrated Circuits and Systems*, 25:274–284, 2006.

[77] Y. Saad and M. Schultz. GMRES: A generalized minimal residual algorithm for solving nonsymmetric linear systems. *SIAM Journal of Scientific and Statistical Computing*, 7:856–869, 1986.

[78] *Matlab v.6*. Mathworks, Inc.

[79] L. Greengard. *The Rapid Evaluation of Potential Fields in Particle Systems*. MIT Press, 1988.

[80] A. H. Boschitsch, M. O. Fenley, and W. K. Olson. A fast adaptive multipole algorithm for calculating screened Coulomb (Yukawa) interactions. *Journal of Computational Physics*, 151:212–241, 1999.

[81] L. N. Trefethen and D. Bau III. *Numerical Linear Algebra*. Society for Industrial and Applied Mathematics, 1997.

[82] K. Nabors and J. White. FASTCAP: A multipole accelerated 3-D capacitance extraction program. *IEEE Transactions on Computer-Aided Design of Integrated Circuits and Systems*, 10:1447–1459, 1991.

[83] S. A. Vavasis. Preconditioning for boundary integral-equations. *SIAM Journal on Matrix Analysis and Applications*, 13:905–925, 1992.

[84] C. M. Stultz. An assessment of potential of mean force calculations with implicit solvent models. *Journal of Physical Chemistry B*, 108:16525–16532, 2004.

[85] S. Jang, E. Kim, and Y. Pak. Free energy surfaces of miniproteins with a $\beta\beta\alpha$ motif: Replica exchange molecular dynamics simulation with an implicit solvation model. *Proteins: Structure, Function, Genetics*, 62:663–671, 2006.

[86] H. Fan, A. E. Mark, J. Zhu, and B. Honig. Comparative study of generalized Born models:

Protein dynamics. *Proceedings of the National Academy of Sciences of the USA*, 102:6760–6764, 2005.

[87] J. Michel, R. D. Taylor, and J. W. Essex. Efficient generalized Born models for Monte Carlo simulations. *Journal of Chemical Theory and Computation*, 2:732–739, 2006.

[88] W. Xin and A. H. Juffer. A boundary element formulation of protein electrostatics with explicit ions. *Journal of Computational Physics*, 2007:416–435, 223.

[89] J. Desmet, M. De Maeyer, B. Hazes, and I. Lasters. The dead-end elimination theorem and its use in protein side-chain positioning. *Nature*, 356:539–542, 1992.

[90] A. R. Leach and A. P. Lemon. Exploring the conformational space of protein side chains using dead-end elimination and the A* algorithm. *Proteins*, 33:227–239, 1998.

[91] R. Geney, M. Layten, R. Gomperts, V. Hornak, and C. Simmerling. Investigation of salt bridge stability in a generalized Born model. *Journal of Chemical Theory and Computation*, 2:115–127, 2006.

[92] R. Zhou and B. J. Berne. Can a continuum solvent model reproduce the free energy landscape of a β-hairpin folding in water? *Proceedings of the National Academy of Sciences of the USA*, 99:12777–12782, 2002.

[93] F. S. Lee and A. Warshel. A local reaction field method for fast evaluation of long-range electrostatic interactions in molecular simulations. *Journal of Chemical Physics*, 97:3100–3107, 1992.

[94] J. A. Board, J. W. Causey, J. F. Leathrum, A. Windemuth, and K. Schulten. Accelerated molecular-dynamics simulatino with the parallel fast multipole algorithm. *Chemical Physics Letters*, 192:89–94, 1992.

[95] C. A. White and M. Head-Gordon. Derivation and efficient implementation of the fast multipole method. *Journal of Chemical Physics*, 101:6593–6605, 1994.

[96] T. C. Bishop, R. D. Skeel, and K. Schulten. Difficulties with multiple time stepping and fast multipole algorithm in molecular dynamics. *Journal of Computational Chemistry*, 18:1785–1791, 1997.

[97] M. Totrov and R. Abagyan. The contour-buildup algorithm to calculate the analytical molecular surface. *Journal of Structural Biology*, 116:138–143, 1996.

[98] J. P. Bardhan, M. D. Altman, J. K. White, and B. Tidor. Numerical integration techniques for curved-panel discretizations of molecule–solvent interfaces. *Journal of Chemical Physics*,

127:014701, 2007.

[99] W. Hackbusch. A sparse matrix arithmetic based on H-matrices. I. Introduction to H-matrices. *Computing*, 62:89–108, 1999.

[100] W. Hackbusch and B. N. Khoromskij. A sparse H-matrix arithmetic. II. Application to multi-dimensional problems. *Computing*, 64:21–47, 2000.

[101] S. Borm, L. Grasedyck, and W. Hackbusch. Introduction to hierarchical matrices with applications. *Engineering Analysis with Boundary Elements*, 27:405–22, 2003.

[102] K. Nabors. *Efficient Three-Dimensional Capacitance Extraction*. PhD thesis, Massachusetts Institute of Technology, 1993.

[103] H. Tjong and H.-X. Zhou. GBr^6: A parameterization-free, accurate, analytical generalized Born method. *JPhysChemB*, 111:3055–3061, 2007.

[104] H. Tjong and H.-X. Zhou. GBr^{6}NL: A generalized Born method for accurately reproducing solvation energy of the nonlinear Poisson–Boltzmann equation. *JChemPHys*, 126:195102, 2007.

[105] V. Z. Spassov, L. Yan, and S. Szalma. Introducing an implicit membrane in generalized Born/solvent accessibility continuum solvent models. *Journal of Physical Chemistry B*, 106:8726–8738, 2002.

[106] W. Im, M. Feig, and C. L. Brooks III. An implicit membrane generalized Born theory for the study of structure, stability, and interactions of membrane proteins. *Biophysical Journal*, 85:2900–2918, 2003.

[107] B. Egwolf and P. Tavan. Continuum description of solvent dielectrics in molecular-dynamics simulations of proteins. *Journal of Chemical Physics*, 118:2039–2056, 2003.

[108] B. Egwolf and P. Tavan. Continuum description of ionic and dielectric shielding for molecular-dynamics simulations of proteins in solution. *Journal of Chemical Physics*, 120:2056–2068, 2004.

[109] R. Zhou, G. Krilov, and B. J. Berne. Comment on "Can a continuum solvent model reproduce the free energy landscape of a β-hairpin folding in water?" The Poisson–Boltzmann equation. *Journal of Physical Chemistry B*, 108:7528–7530, 2004.

[110] D. Beglov and B. Roux. Finite representation of an infinite bulk system: Solvent boundary potential for computer simulations. *Journal of Chemical Physics*, 100:9050–9063, 1994.

[111] J.-H. Lin, N. A. Baker, and J. A. McCammon. Bridging implicit and explicit solvent ap-

proaches for membrane electrostatics. *Biophysical Journal*, 83:1374–1379, 2002.

[112] M. S. Lee, F. R. Salsbury, Jr., and M. A. Olson. An efficient hybrid explicit/implicit solvent method for biomolecular simulations. *Journal of Computational Chemistry*, 25:1967–1978, 2004.

[113] G. Brancato, N. Rega, and V. Barone. Reliable molecular simulations of solute–solvent systems with a minimum number of solvent shells. *Journal of Chemical Physics*, 124:214505, 2006.

[114] Y. Li, G. Krilov, and B. J. Berne. Elastic bag model for molecular dynamics simulations of solvated systems: Application to liquid water and solvated peptides. *Journal of Physical Chemistry B*, 110:13256–13263, 2006.

NOTICE

List of Figures

Figures

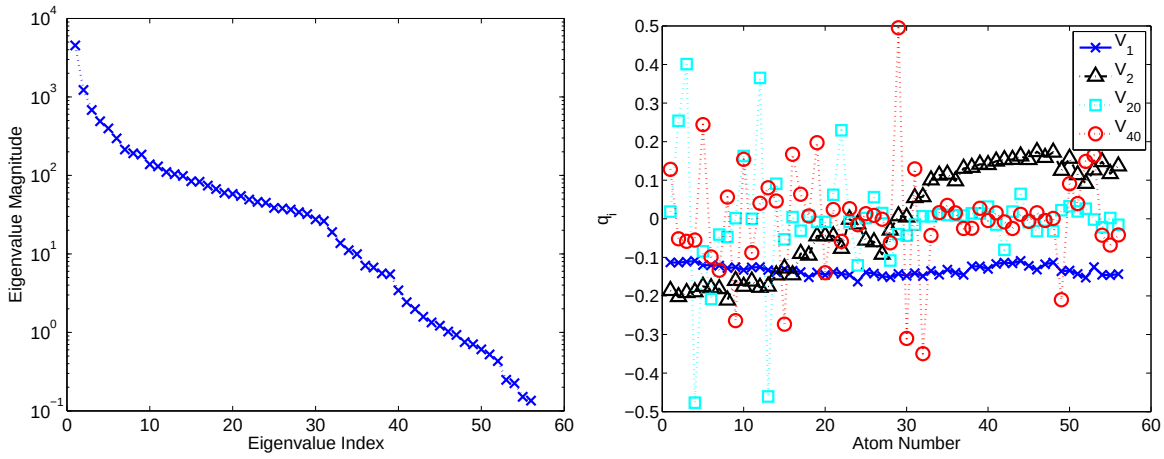

(a) (b)

FIG. 1: The eigendecomposition of the tripeptide reaction-potential matrix calculated using boundary-element methods. (a) The eigenvalues of M_{BEM}. (b) Selected eigenvectors of M_{BEM}, plotted as a function of atom number.

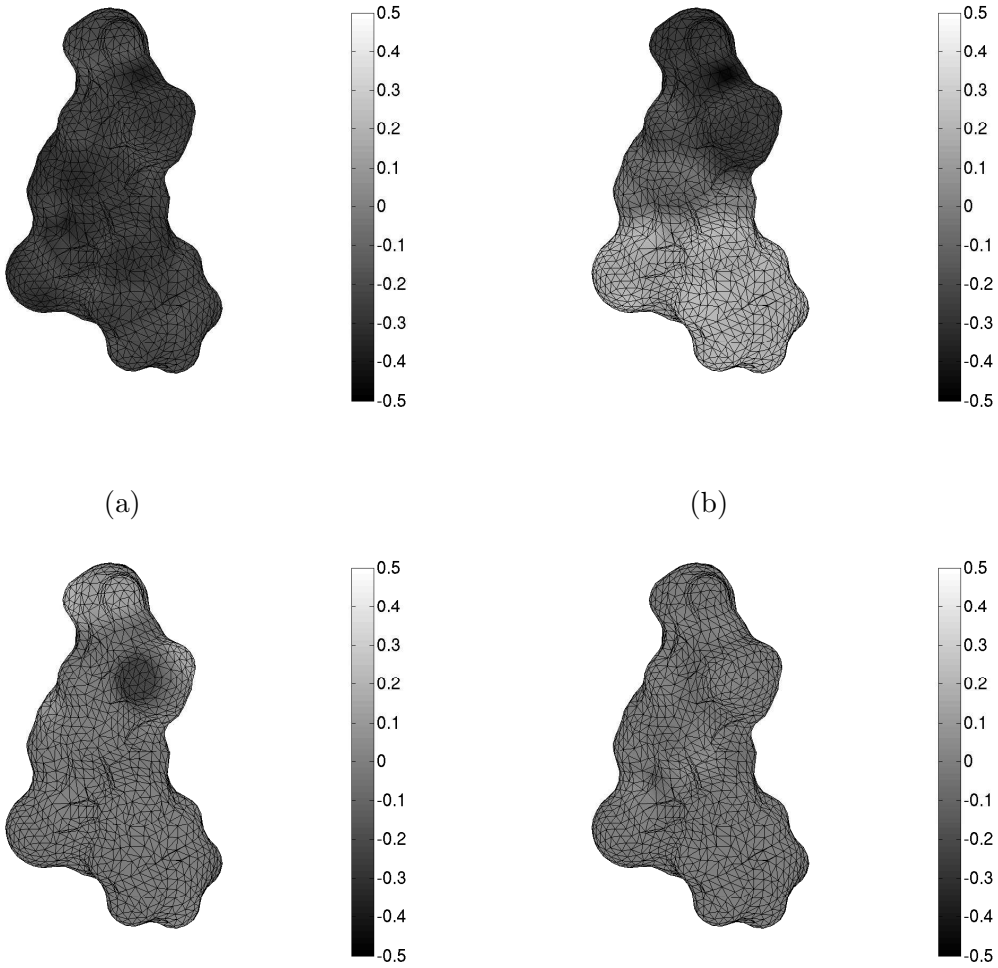

FIG. 2: The normal component of the electric displacement field at the boundary of a tripeptide given different charge distributions q. (a) $q = V_1$. (b) $q = V_2$. (c) $q = V_{20}$. (d)$q = V_{40}$.

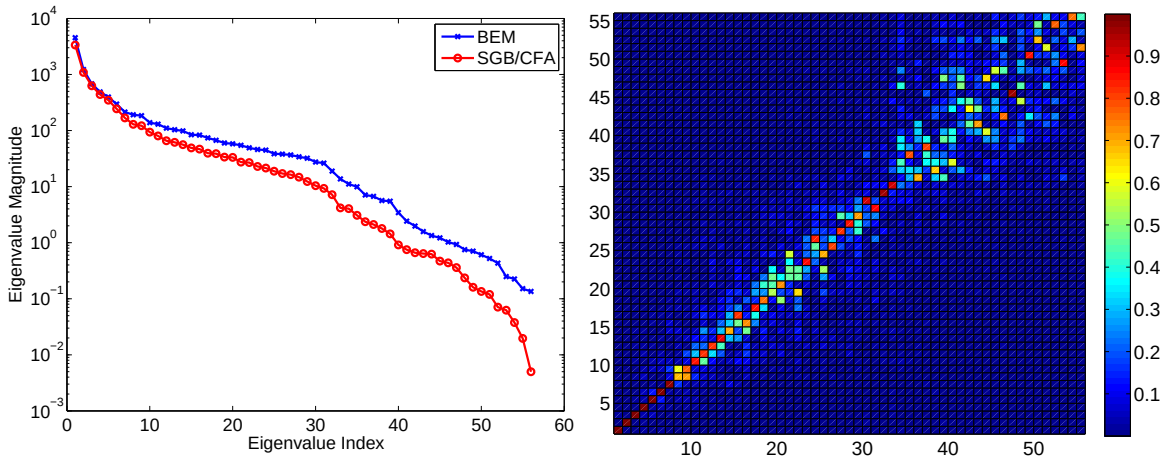

FIG. 3: Comparison of the eigenvectors and eigenvalues of the reaction-potential matrices calculated by BEM and surface-integration methods for calculating effective Born radii using only the Coulomb-field approximation (equivalent to the surface generalized-Born method of Ghosh *et al.* but without the empirical corrections used in that work) [31].

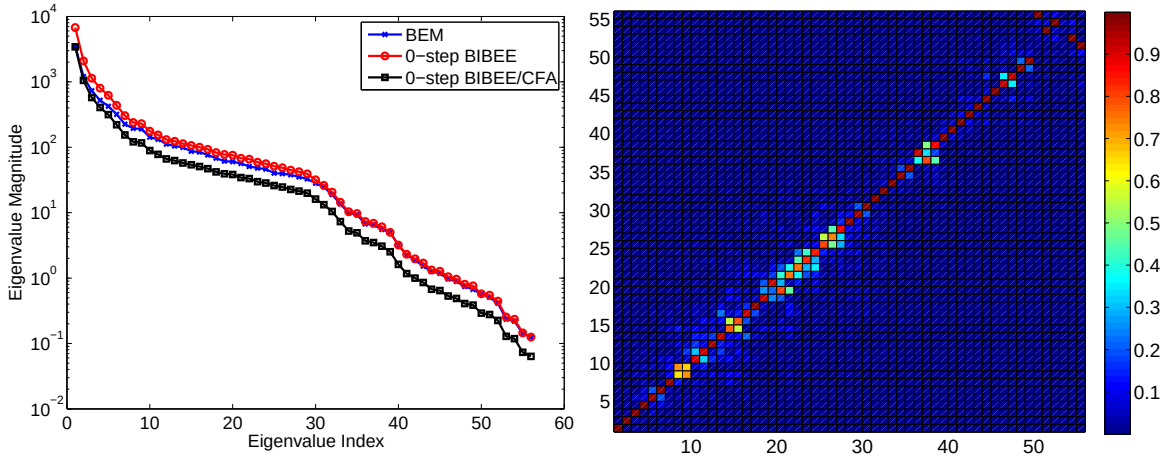

(a) (b)

FIG. 4: Comparison of the eigenvectors and eigenvalues of the reaction-potential matrices calculated by BEM and the 0-step BIBEE method.

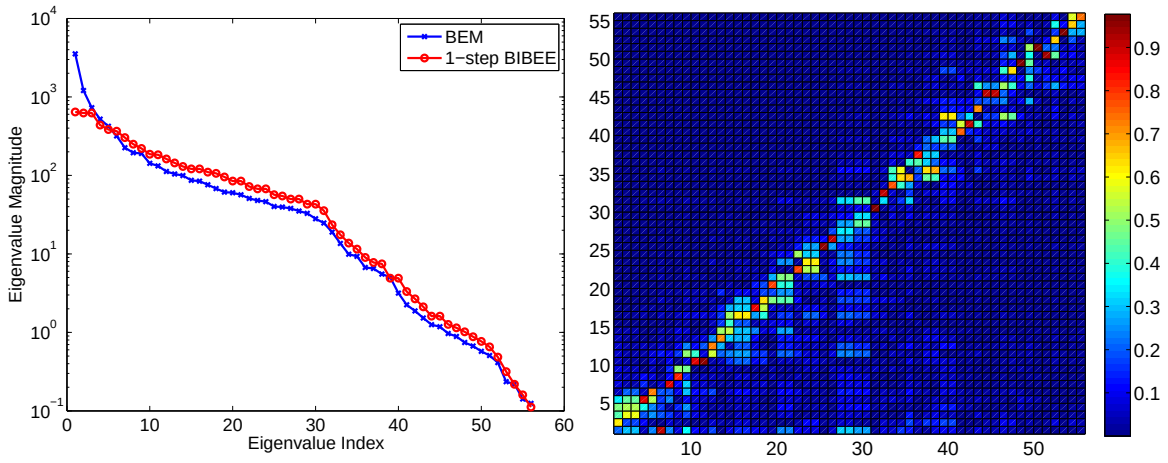

(a) (b)

FIG. 5: Comparison of the eigenvectors and eigenvalues of the reaction-potential matrices calculated by BEM and the 1-step BIBEE method.

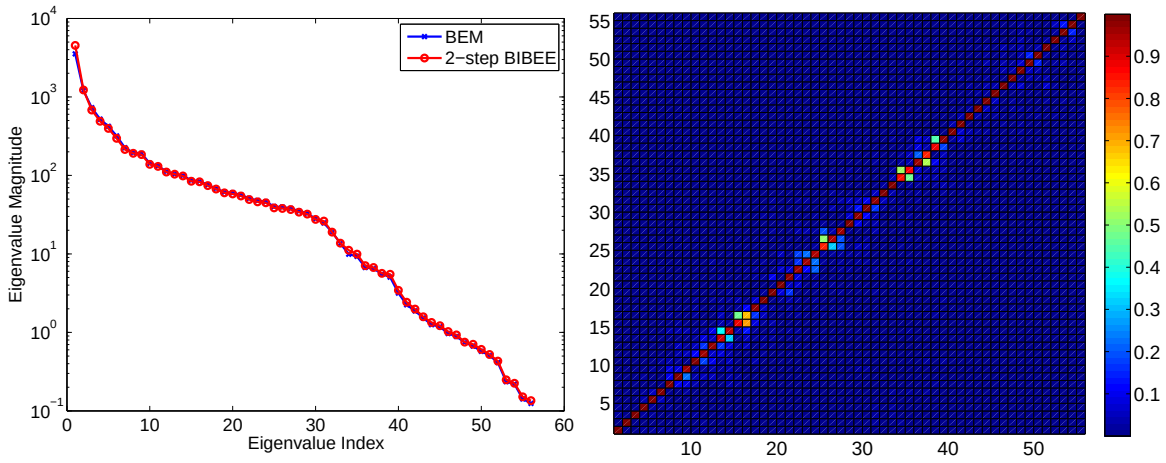

(a) (b)

FIG. 6: Comparison of the eigenvectors and eigenvalues of the reaction-potential matrices calculated by BEM and the 2-step BIBEE method.

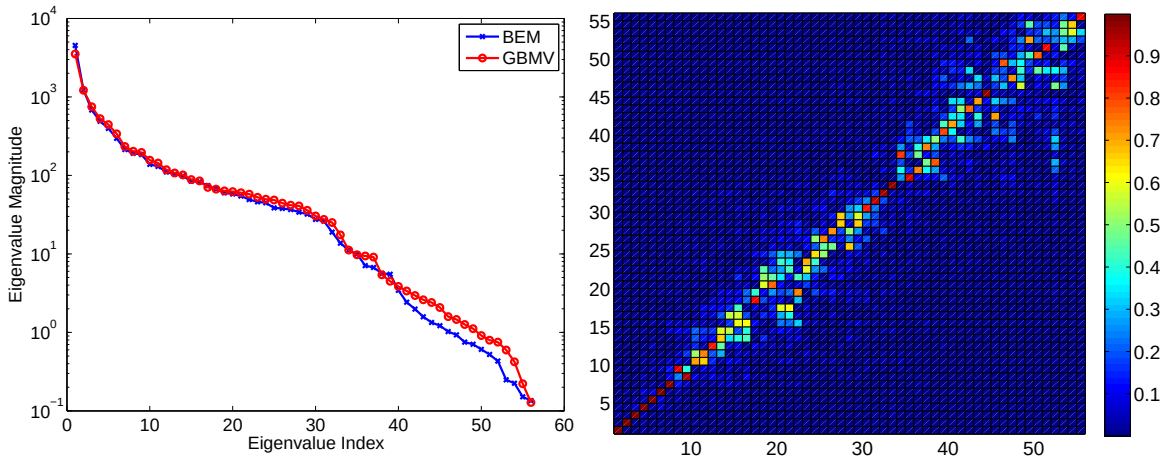

FIG. 7: Comparison of the eigenvectors and eigenvalues of the reaction-potential matrices calculated by BEM and GBMV [25].